HEDL-SA-1705

CONF-790366--1

EXPERIMENTAL ELECTRO-THERMAL METHOD FOR NONDESTRUCTIVELY TESTING WELDS IN STAINLESS STEEL PIPES

MASTER

D. R. Green

January 19, 1979

HANFORD ENGINEERING DEVELOPMENT LABORATORY
Operated by Westinghouse Hanford Company, a subsidiary of Westinghouse Electric Corporation, under the Department of Energy Contract No. EY-76-C-14-2170

DISCLAIMER

EXPERIMENTAL ELECTRO-THERMAL METHOD FOR NONDESTRUCTIVELY TESTING WELDS IN STAINLESS STEEL PIPES

By

D. R. Green

1. INTRODUCTION

Welds in austenitic stainless steel pipes are notoriously difficult to nondestructively examine using conventional ultrasonic and eddy current methods. Surface irregularities and microscopic variations in magnetic permeability cause false eddy current signal variations. Ultrasonic methods have been developed which use computer processing of the data to overcome some of the problems [1,2]. Electro-thermal NDT (nondestructive testing) shows promise for detecting flaws that are difficult to detect using other NDT methods. This paper describes results of a project completed to develop and demonstrate the potential of an electro-thermal method for nondestructively testing stainless steel pipe welds.

Electro-thermal NDT uses a brief pulse of electrical current injected into the pipe. Defects at any depth within the weld cause small differences in surface electrical current distribution. These cause short-lived transient temperature differences on the pipe's surface that are mapped using an infrared scanning camera. Localized microstructural differences and normal surface roughness in the welds have little effect on the surface temperatures.

The most important objective in the present work was development of practical contacts for injecting the electro-thermal exciting current into as-received stainless steel pipe weld specimens without contaminating or damaging the surface. Another objective was to demonstrate the electro-thermal methods's potential applicability to stainless steel welds of the type used in FFTF (Fast Flux Test Facility) pipes. This differs from past work since the previous efforts were aimed at initital sensitivity demonstrations on carbon steel bars and welds [3,4] and flat stainless steel plates [5]. Hence contacts for injecting current into test specimens in the past work were primative, consisting of copper bars or plates that were simply clamped or bolted to the surface of the test specimens with little concern for surface contamination or damage. Contacts developed during the present work were required to make electro-thermal NDT a potentially practical method for stainless steel pipe welds.

2. BASIC PRINCIPLES

Low frequency electrical current, injected at widely separated points on the surface of a pipe, distributes itself throughout the thickness of the pipe wall. Most of the total current is concentrated between the injection electrodes as shown in Figure 1. The electrical current's depth of penetration can be controlled to give either complete penetration or concentration near the surface by simply adjusting the spacing between electrodes as illustrated in Figure 2. The electrical current frequency could also be used to control penetration (skin depth), but would require a more expensive supply system. Reducing the penetration properly can make the outside surface current density nearly independent of conditions such as drop-through on the inside surface of a pipe weld, while at the same time retaining sensitivity to defects penetrating 20% or more of the way into the weld from the inside surface.

Normal outside surface contour over the weld zone has only a small effect on the surface current density pattern since the current tends to follow the contour as illustrated in Figure 3A. A flaw, on the other hand, has a large effect on the surface current density pattern, as shown in Figure 3B. Only the component of current flowing perpendicular to planar flaws would have an effect, so several electrode placements would be used when this type of flaw is expected.

Since the electrical current conforms to the test object, complex shapes can be nondestructively tested using the electro-thermal method. For example, a nozzle assembly or pipe "T" which is difficult to examine using conventional NDT methods could easily be examined using the electro-thermal method as illustrated in Figure 4.

The instantaneous electrical heat production at any point in a metal is proportional to the square of the current density at that point. The large localized increase in the current density at the outer surface of the pipe over a flaw causes a warm spot in the surface temperature map at that location. An infrared scanning camera (hereafter called a scanner) can be used to produce a visible picture of the temperature map in which warmer regions are brighter and cooler regions are darker. An intense, short pulse of current and a high speed infrared scanner are required for best results. Transient temperature differences of a few degrees centigrade over small flaws in metal are short-lived due to the high thermal diffusivity. Rapid diffusion of heat causes temperature differences around localized minute differences in microstructure to be "washed out", while those resulting from macroscopic flaws are retained. A typical electrical heating pulse length used in stainless steel is 100 milliseconds. The infrared scan should be completed within 60 milliseconds or less after termination of the heating pulse.

For further discussion of the basic principles of electro-thermal NDT, the reader is referred to earlier work on the subject [3-5].

3. CURRENT INJECTION CONTACT ASSEMBLIES

Contacts that permit injection of a high current without damaging or contaminating the pipe surface are essential. This requires uniform, low resistance contact between the current injection electrodes and the surface of the stainless steel pipe. The contact assemblies for this purpose must produce good contact at pressures low enough to avoid any possibility of mechanical damage to the pipe. Electrical resistivity of the contact materials must be low to prevent overheating of the contacts from resistance heating in the materials themselves. Finally, the electrical field produced at the pipe surface under the contacts must be properly shaped to avoid excessive field gradients at and near the inner edges of the contacts. Otherwise, the local current density can become so large that it causes burning and pitting along the inner edge of the contact. Field shaping is accomplished by inserting an insulating strip along the top inside portion of the contact assembly as shown in cross section in Figure 5. The electrical field gradient that is highly concentrated at the inner edge of the contact in Figure 5A is more evenly distributed in Figure 5B due to resistive drops through the longer path around the insulator for current flowing to the inner edge of the contact.

Uniform contact between the electrodes and pipe surface at low contact pressures requires a highly pliable contact that will easily comply with normal small irregularities on the pipe surface. At the same time, the pipe surface must be protected from contact with soft metals. To accomplish this, a 0.005 inch (0.013 cm) thick stainless steel foil was placed against the pipe surface. A copper electrode curved to match the pipe curvature was used to apply pressure to the stainless steel foil through a fully annealed 0.125 inch (0.013 cm) thick layer of aluminum. The contact pressure required can be further reduced by applying the aluminum pressure pad at a high temperature to soften it. All hot as well as cold pressure pads used in the present work were either type 1100 commercial grade, or 99.99% pure aluminum. Figure 6 shows a cross sectional view of the contact assemblies in relationship to the pipe weld and electrodes. Although time did not permit experimental evaluation of ordinary commercial purity heated aluminum pressure pads, basic considerations show that low contact pressures could be used with them.

4. EXPERIMENTAL METHODS AND EQUIPMENT

Early electro-thermal experiments to demonstrate the detectability of defects in stainless steel pipe welds used electrodes that were silver soldered directly to the pipe. Since soldered electrodes eliminate effects of contact resistance, results obtained with them provided a valuable comparison with results obtained later with surface contacts. Figure 7 shows a stainless steel pipe weld specimen with silver soldered electrodes set up and ready for an electro-thermal experiment. Discoloration of the specmen was caused by the heat used to silver solder the electrodes; the temperature rise of a few degrees during electro-thermal NDT does not cause any discoloration. The round nose of the infrared scanning camera can be seen at the bottom of Figure 7. A rear view of the specimen/electrode assembly is shown in Figure 8. An EDM (Electro-Discharge Machined) defect purposely introduced into the weld from the back (inside) surface can be seen a small distance below the center of the sample. A schematic diagram describing the configuration and nonemclature of the pipe weld specimens and EDM produced defects used in early experiments with soldered electrodes as well as later experiments with non-bonded contacts is shown in Figure 9. All of these defects were 1-cm long.

Surface contacts of the type described in Section 3 were used with the laboratory electro-thermal NDT system shown in Figure 10. A small laboratory press seen in the center of the figure, was used to apply known pressures to the contacts during experiments. In the foreground (upper right) of the figure the infrared scanner can be seen. The scanner views the stainless steel pipe weld surface through an opening in the top of the upper press platten by means of a first-surface mirror tilted at 45 degrees, as seen in Figure 10 and 11. A timing system used to control the 100 millisecond heating current pulse and camera shutter can be seen at the operator's left side in Figure 10. The current pulse was supplied by a small 13 inch x 19 inch x 20 inch (33 cm x 48 cm x 51 cm) transformer capable of a 6 volt RMS output at a maximum current of approximately 20K amps. Input voltage amplitude to the transformer was controlled with a variac stack and switched on and off with a contactor. Solid state devices such as silicon controlled rectifiers can also be used for the switching and voltage control.

Figure 11 shows one of the contact assemblies being inserted between an electrode and the stainless steel pipe weld specimen. Electrodes and contact assemblies are shown in-place and ready for electro-thermal NDT of a weld specimen cut from a 14-inch (36 cm) diameter austenitic stainless steel pipe in Figure 12. To reduce the criticality of alignment and improve the uniformity of contact pressure distribution, an electrode assembly designed to swivel at three locations was applied as shown in Figure 13.

Connectors on flexible cables used to supply current to the electrodes can be seen bolted to copper rails on each side of the swivel electrode assembly. The contacts used with this assembly were designed to be preheated by passing a current through the aluminum pressure pads prior to making contact with either the electrodes or the stainless steel pipe. Copper bar conductors and clamps to supply current for heating the pressure pads are seen in the foreground and background in Figure 13. After heating, the contact assemblies were quickly clamped to the pipe surface with a pneumatic cylinder. Rapid clamping was required since temperatures within the thin aluminum pressure pads drop below the desired level in milliseconds after contact with the pipe surface and copper electrode. (Pre-heating the copper could not be used since it would then form a heavy oxide coating). Heating current applied to the aluminum pressure pads ranged from 1000 to 2000 amperes.

5. RESULTS AND INTERPRETATION

Electro-thermal NDT data from the stainless steel pipe weld specimens was recorded directly as thermographic maps of the surface temperature immediately following a 0.1 second pulse of electrical current that was passed through the test specimen. Bright areas in these maps are warmer than the surrounding darker areas.

Figure 14 shows results that were all obtained from the single stainless steel pipe weld specimen having silver-soldered electrodes (shown in Figures 7 and 8). This data is included for comparison with later results obtained using surface contacts. The EDM-produced weld defect (seen in Figure 8) had not yet been cut into the weld when the results shown in Figure 14A were obtained. Results shown in Figure 14B, C and D were obtained after the defect was electro discharge machined to depths of 43, 66, and 100% respectively, of the weld zone thickness (see Figure 9). In the center of each thermal map over the defect is a bright (warm) spot which increases the brightness as the defect gets closer to outside (scanner-viewed) surface. In Figure 14(D) where the defect had been machined through the outside surface, a bright flare appears at the ends of the defect. Dark regions appear on both sides of the defect as expected on the basis of previous work [4]. The bright strips on both sides of the weld zone in all four temperature maps in Figure 14 are warm regions resulting from the pipe wall being 25% thinner than the weld zone. Although the limited latitude of the photographic process causes detail in these areas to be washed-out, the electronic signal-to-noise ratio was high. Hence, defects at the edges of the weld should be detectable with the infrared scanner's brightness adjusted to a lower level.

Background brightness differences due to the large, relatively predictable thickness change at the edges of the weld can be subtracted from the temperature maps in a manner similar to that used in subtracting or discounting the effect of thickness changes in radiographs of welds. Three methods by which the electro-thermal data might be approximately compensated for gross weld thickness effects are:

1) measure the height of the weld crown above the adjacent pipe surface, assume it is the total thickness change and compensate accordingly,

2) assume circumferential symmetry (at least locally) in the weld around the pipe and test for sudden defect-caused differences in circumferential electro-thermal map symmetry, and

3) use a through-the-pipe radiograph to determine pipe weld thickness differences when 1) and 2) yield confusing results.

Another effect that must be considered in interpreting the electro-thermal results is the effect of abrupt breaks in surface countour where the outer edge of a high-crowned weld meets the pipe weld. If the obtuse angle at the intersection of the weld crown and pipe wall is too small, it can cause a slightly higher local heat generation. It should be possible to compensate the electro-thermal results for this effect by measuring the angle of intersection and using it to determine the correction in temperature profile.

The pliable surface contacts (non-bonded) were used with the apparatus shown in Figures 10-12 to obtain the electro-thermal results shown in Figure 15. Note the similarity between these results and those obtained with soldered contacts. With the surface contacts, however, it was possible to determine the effects of electrode spacing in addition to the effect of defect depths since the electrodes were movable. In Figure 15A, the defect indication increases in intensity as the defect's depth into the weld from the inside surface increases. Figures 15B and 15C show the effect of electrode spacing on detection of defects penetrating 20 and 50%, respectively, into the weld from the inside surface. An electrode spacing of 3.8 cm was optimum for detection of the 20% defect. This was reasonable, since the current penetration depth is too small to reach the defect when small electrode spacings are used, and large electrode spacings cause specimen resistance and parallel leakage currents too high to allow adequate current density between the electrodes. Results for the 50% defect (see Figure 15C) confirm the effect of large spacing since a more intense defect indication is obtained with a 2.5 cm spacing than with a 3.8 cm spacing. If the current density between electrodes were equal for both spacings, a more intense indication would be expected with the larger spacing since the current penetration depth would be larger and therefore more affected by the defect.

Several parameters have a significant effect on the surface temperature map produced during a test. Defect length as well as depth can be important. Surface emissivity of the pipe is not important in a heavily oxidized weld zone, such as the one in the pipe specimen with soldered electrodes. However, in bright or lightly oxidized welds emissivity variations could have an effect and must be eliminated. Fast Flux Test Facility stainless steel pipe welds are normally wire brushed with a stainless steel brush. Weld specimens for the experiments using flexible non-bonded contacts were prepared in this way and were bright and shiny. An automatic emissivity independent infrared NDT method is available [6]. However, in these experiments, a simple technique employing a flat black coating to eliminate surface emissivity effects was used. Care was taken not to get any of the coating on the pipe where the contacts were to be placed.

Surface contact pressures required to avoid pitting and burning of stainless steel pipe surface were determined by repeatedly testing the pipe weld specimens using a 20K amp current pulse. The pressure used in each subsequent test was decreased until signs of surface pitting and burning were noted. Results of these tests showed that contacts using commercial grade type 1100 aluminum pressure pads operated satisfactorily when pre-loaded to 10,000 lb/in^2 (703 Kg/cm^2) and subsequently clamped at 5000 lb/in^2 (352 Kg/cm^2). Annealed, high purity aluminum (99.99%) pressure pads made it possible to eliminate the pre-load. However, with a simple fixed-electrode system, a contact pressure of 5000 psi was necessary even with high purity aluminum pads. A few tests using the swivel electrode assembly (see Figure 13) indicated that contact pressures down to approximately 1000 psi (70 Kg/cm^2) could be successfully used with the high purity aluminum pressure pads.

Contact assemblies gave the best results when the aluminum pressure pads were annealed before each use. Stainless steel isolator foils 0.0005 inch (0.013 cm) thick were placed between the aluminum pressure pads and surface of the stainless steel pipe in all of the experiments using surface contact current injection.

As mentioned earlier, the aluminum pressure pads are softer when they are hot. This reduces the pressure required to make the aluminum comply with the pipe surface. Hot, high purity aluminum pressure pads were used in contact assemblies during two experiments in which the pads were preheated to approximately 600°F (316°F). A pneumatic press quickly moved the hot contacts to the pipe surface and then compressed the aluminum presure pads to their final seating in 1 to 2 milliseconds. The speed of final compression is important since otherwise heat transfer from the pressure pad through the stainless steel isolator foil into the pipe wall would cool the pad before the compression was complete. Pressures down to the minimum limit of the press, 1750 psi (123 Kg/cm^2), were successfully used with the contacts on an as-received stainless steel pipe weld specimen without damage from the current pulse. Time did not permit modifying the press to allow experiments at lower contact pressures.

6. CONCLUSIONS AND RECOMMENDATIONS

This work has demonstrated the potential of the electro-thermal method for nondestructively testing austenitic stainless steel pipe welds. The new contact assemblies developed for injecting current into the the welds during electro-thermal NDT have a current carrying a capacity of at least 20,000 amperes/in^2 (3100 amperes/cm^2) without pitting or burning. These contacts do not contaminate the pipe surface since the only parts touching the pipe are the stainless steel isolator foils. They were successfully tested at clamping pressures down to 1000 psi which should be low enough to be safely used on stainless steel pipe. Even lower pressures may be acceptable, especially with heated contacts, but further experiments are needed to explore this.

The minimum detectable EDM-produced defect depth using the present equipment under laboratory conditions appears to be about 20% penetration from the inside surface of the weld, assuming the electro-thermal equipment is being applied at the outside surface. The basic principles involved in electro-thermal NDT indicate that an open natural defect will give about the same results as an EDM-produced defect of the same size and geometry. Determining the minimum detectable defect size under field conditions will require implementation of three features that were beyond the scope of the present equipment. These are:

1) Procurement of a large pulsed current supply practical for portable field use in electro-thermal NDT of stainless steel pipe and pipe welds.

2) A data collection and analysis method that will allow computer evaluation of tests results.

3) An emissivity correction system to allow application to stainless steel pipe welds in an as-found condition, rather than requiring that the welds be coated.

The emissivity correction process will add noise to the defect detection signals. However, this can be at least partially offset by using a scanner having a better signal-to-noise ratio.

Although the scope of the present work included dozens of electro-thermal tests during the development and evaluation of the new contacts on stainless steel pipe welds, further work is needed to evaluate the effects of a wide variety of conditions that will be encountered during field tests. A full evaluation will require hundreds of tests on different stainless steel pipe welds. Evaluations included in the present work strongly indicate the electro-thermal method will detect defects in the as-cast region of stainless steel pipe welds that are difficult to detect by any other existing NDT method. In addition, this method should be useful for application to complex shapes as pipe tees, nozzles, fillet welds and complicated castings.

REFERENCES

(1) S.J. Mech and T.E. Michaels, "Development of Ultrasonic Examination Methods for Austenitic Stainless Steel Weld Inspection", Materials Evaluation, pp. 81-86, July, 1977.

(2) M.R. Hill, Nondestructive Testing Development Program Quarterly Report for Period Ending September 30, 1978, ORNL-5490, December, 1978.

(3) D.R. Green and L.D. McCullough, An Electro-Thermal Nondestructive Testing Method, BNWL-1273, December, 1969.

(4) L.D. McCullough and D.R. Green, "Electro-Thermal Nondestructive Testing of Metal Structures", Materials Evaluation, pp. 87-91 April, 1972.

(5) D.R. Green and J.A. Hassburger, "Infrared Electro-Thermal Examination of Stainless Steel", Materials Evaluation, pp. 39-43, 50, March, 1977.

(6) D.R. Green, "Emissivity Independent Infrared Thermal Testing Method", Materials Evaluation, pp. 79-85, February, 1965.

ACKNOWLEDGEMENTS

It is a pleasure to acknowledge the work of D. R. Maley in engineering and directing as well as performing many of the experiments. The engineering, design and procurement work of R. J. Quon on the swivel electrode and pneumatic press system, and the laboratory assistance of R. B. Erickson is gratefully acknowledged. This work was performed under the Department of Energy Contract No. EY-76-C-14-2170.

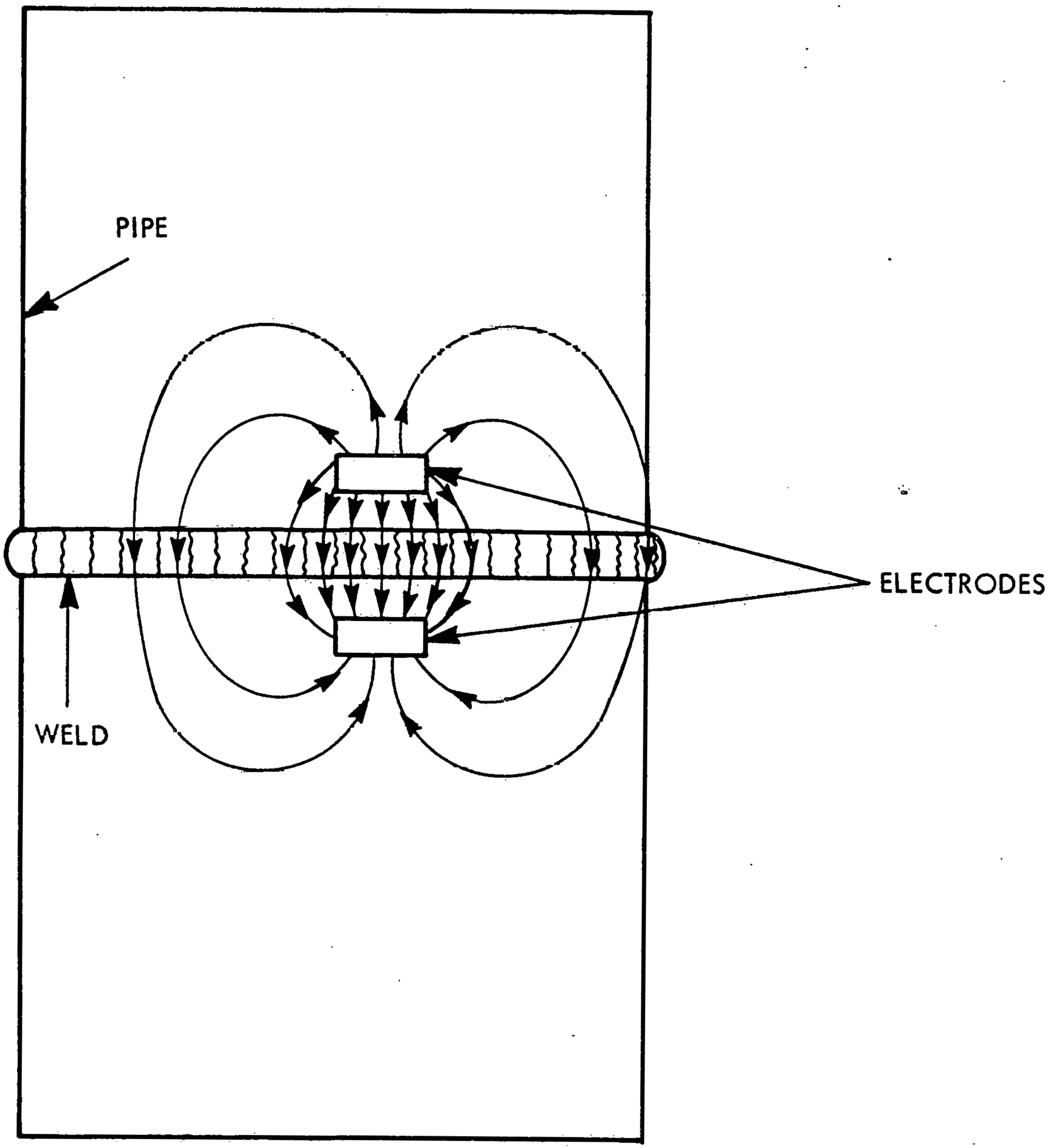

HEDL 7901-101.3

Figure 1. Electrical current flow between small electrodes on the outer surface of a pipe.

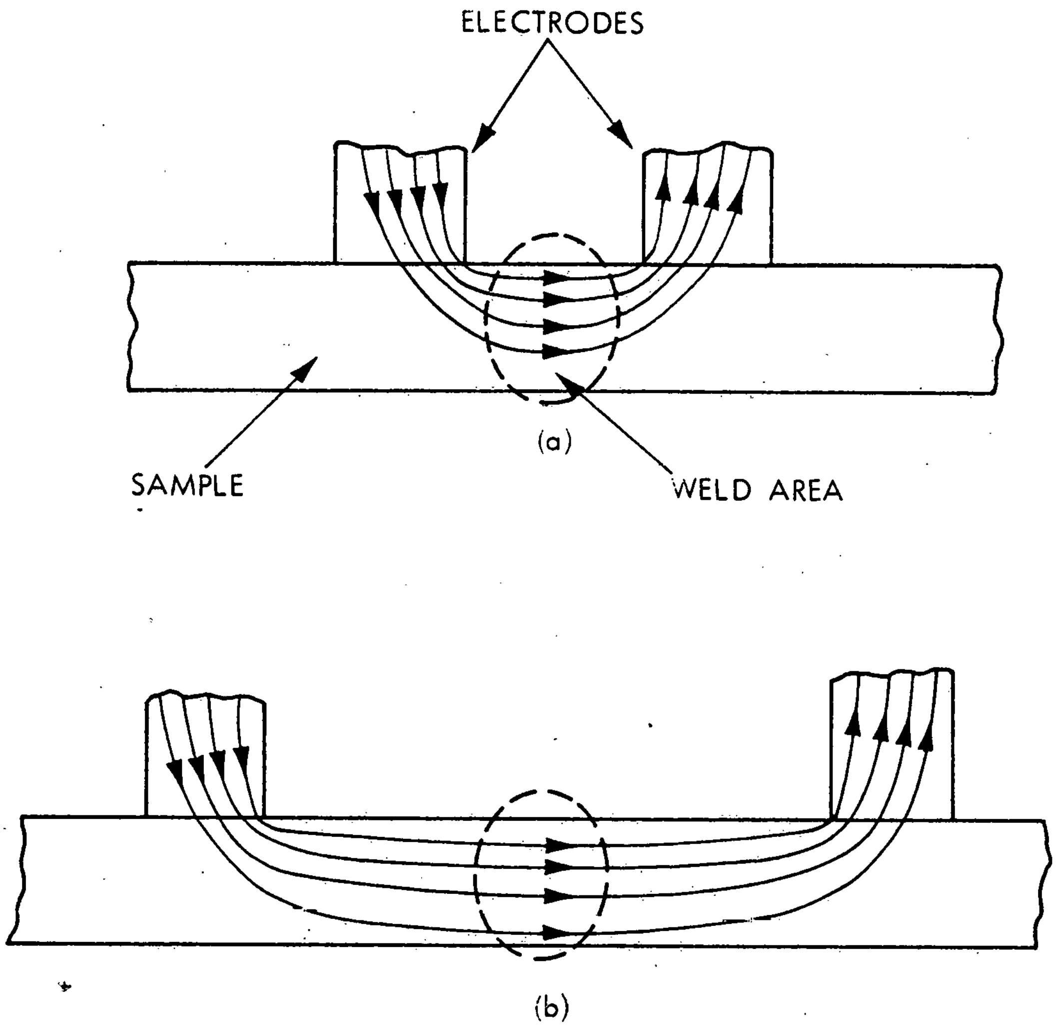

HEDL 7806-251.2

Figure 2. (A) Closely spacing electrodes reduces penetration depth of the electrical current.

(B) Widely spacing electrodes increases penetration depth of the electrical current.

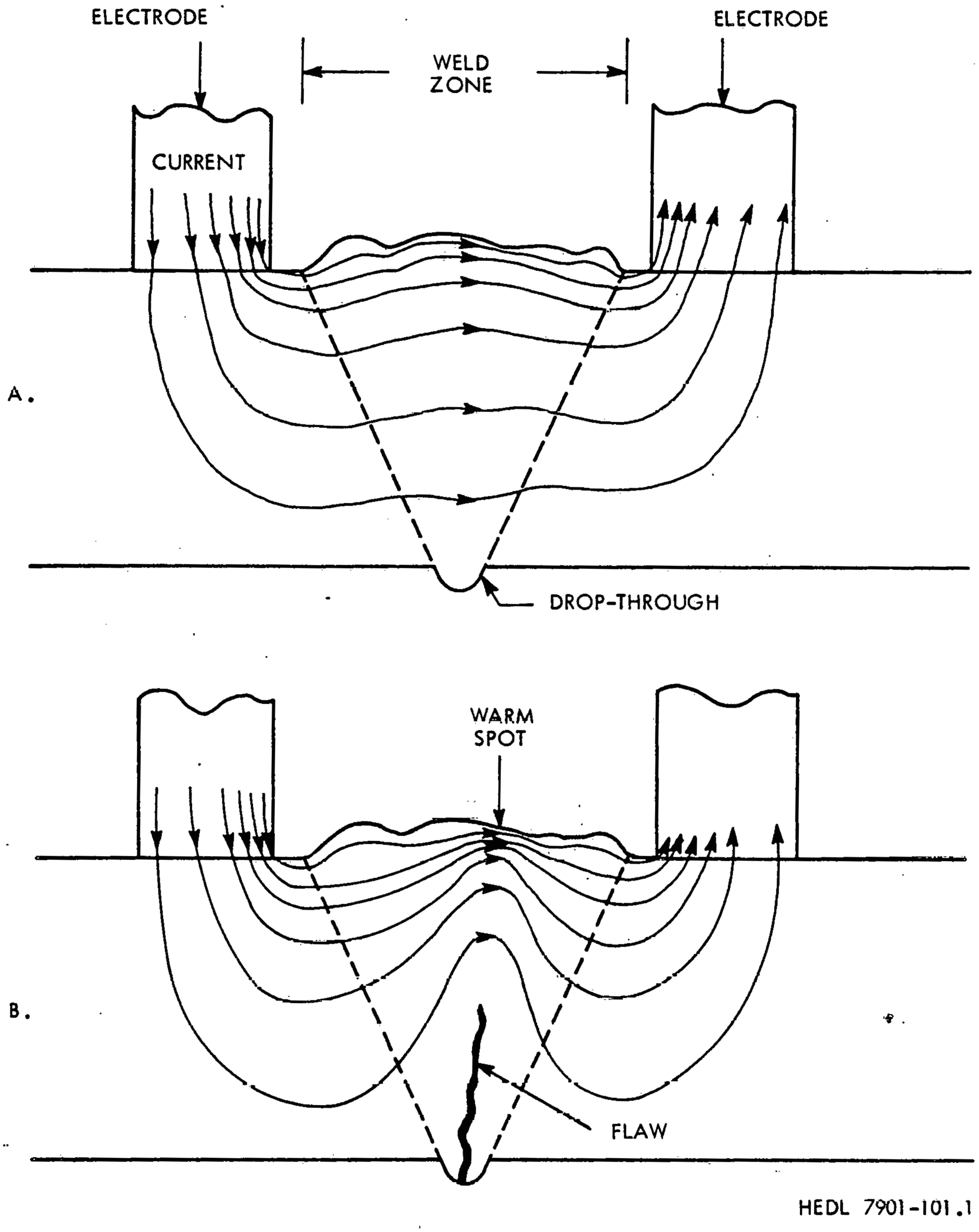

Figure 3. A. Current flow tends to follow surface contour over the weld zone.

B. Flaw in weld zone has a much larger effect than surface contour on the current distribution.

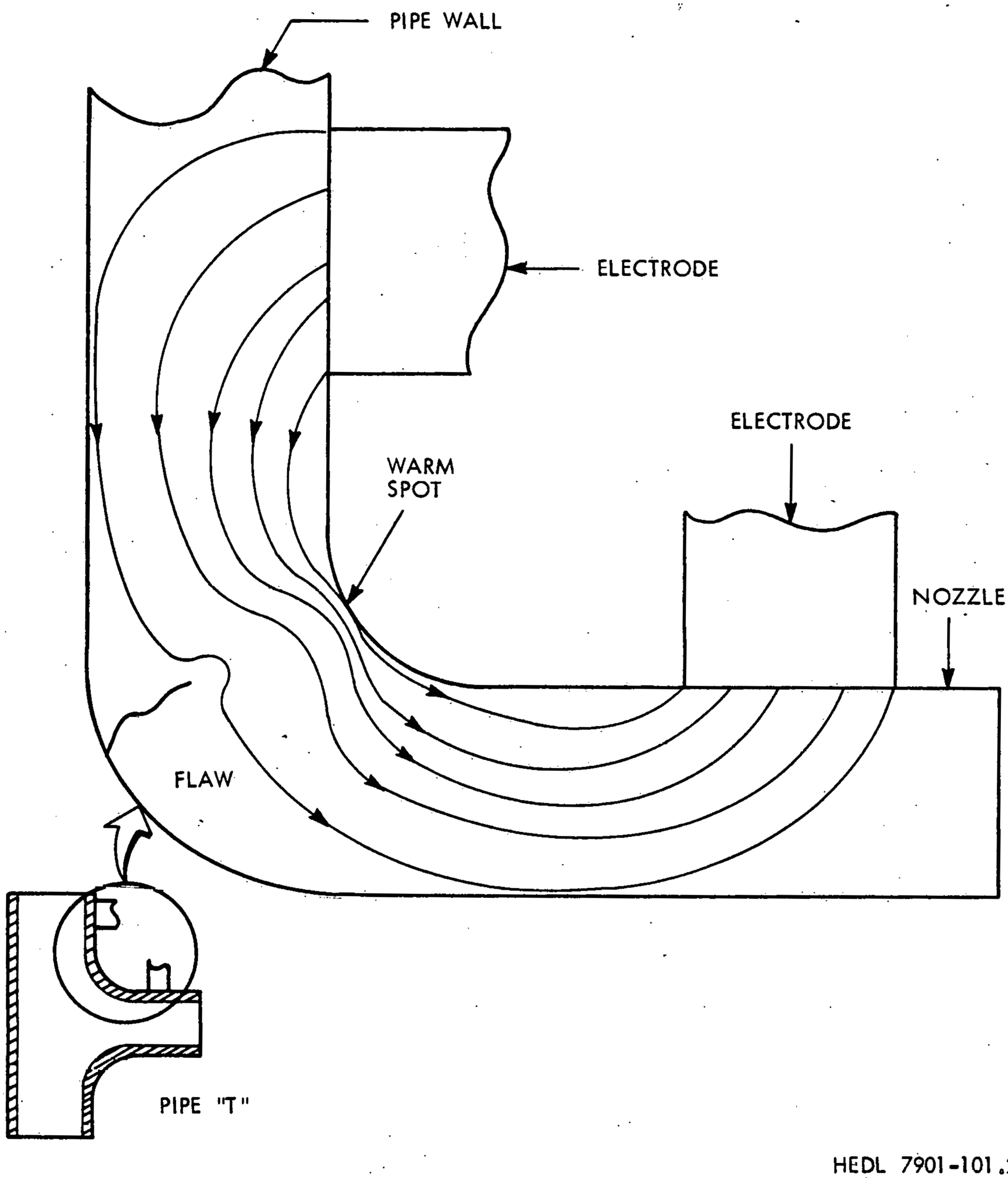

Figure 4. Complex shapes can be nondestructively tested using the electro-thermal method.

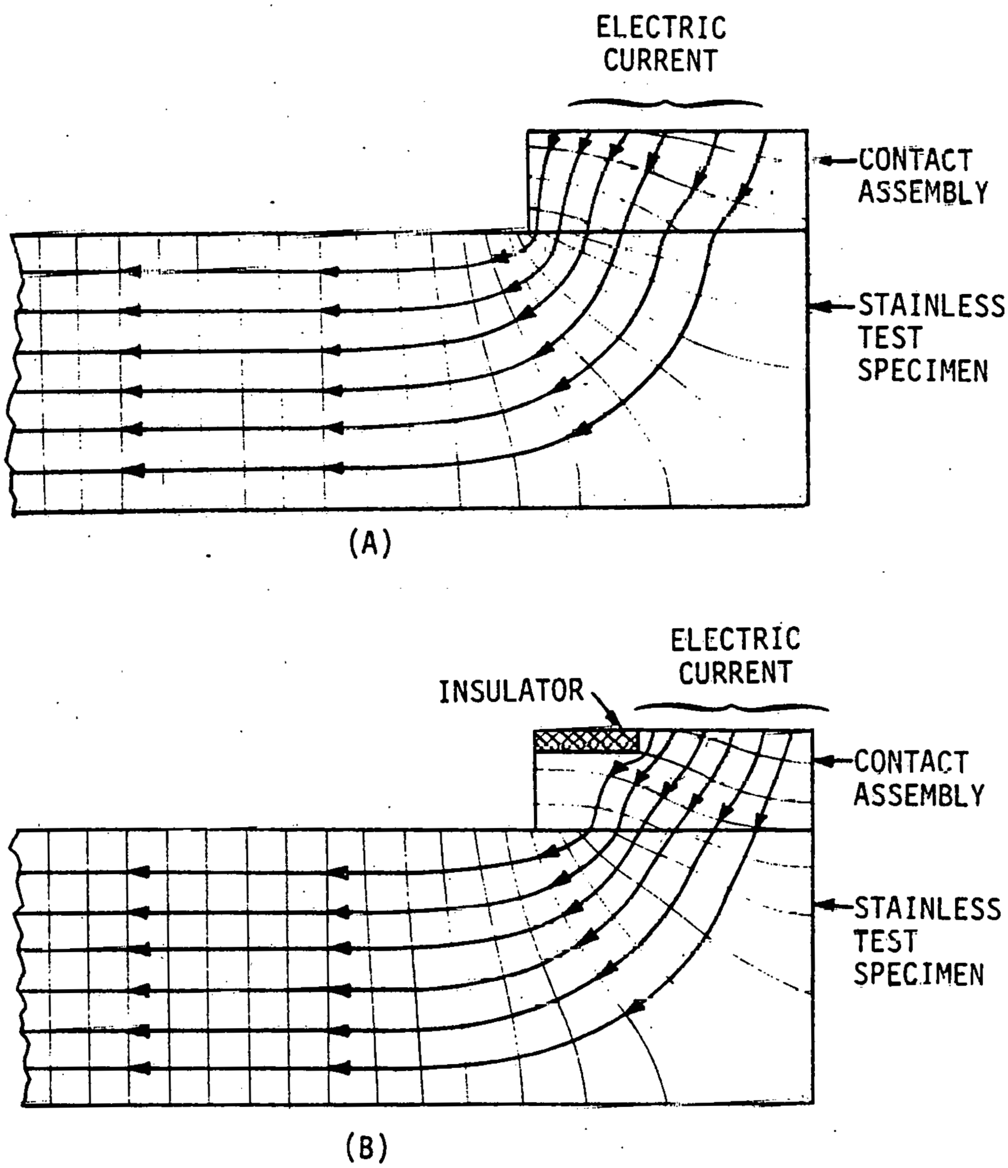

Figure 5. Schematic Illustration of Electrical Current in the Contact and Test Specimen: (A) Without and (B) With Field Shaping Insulator.

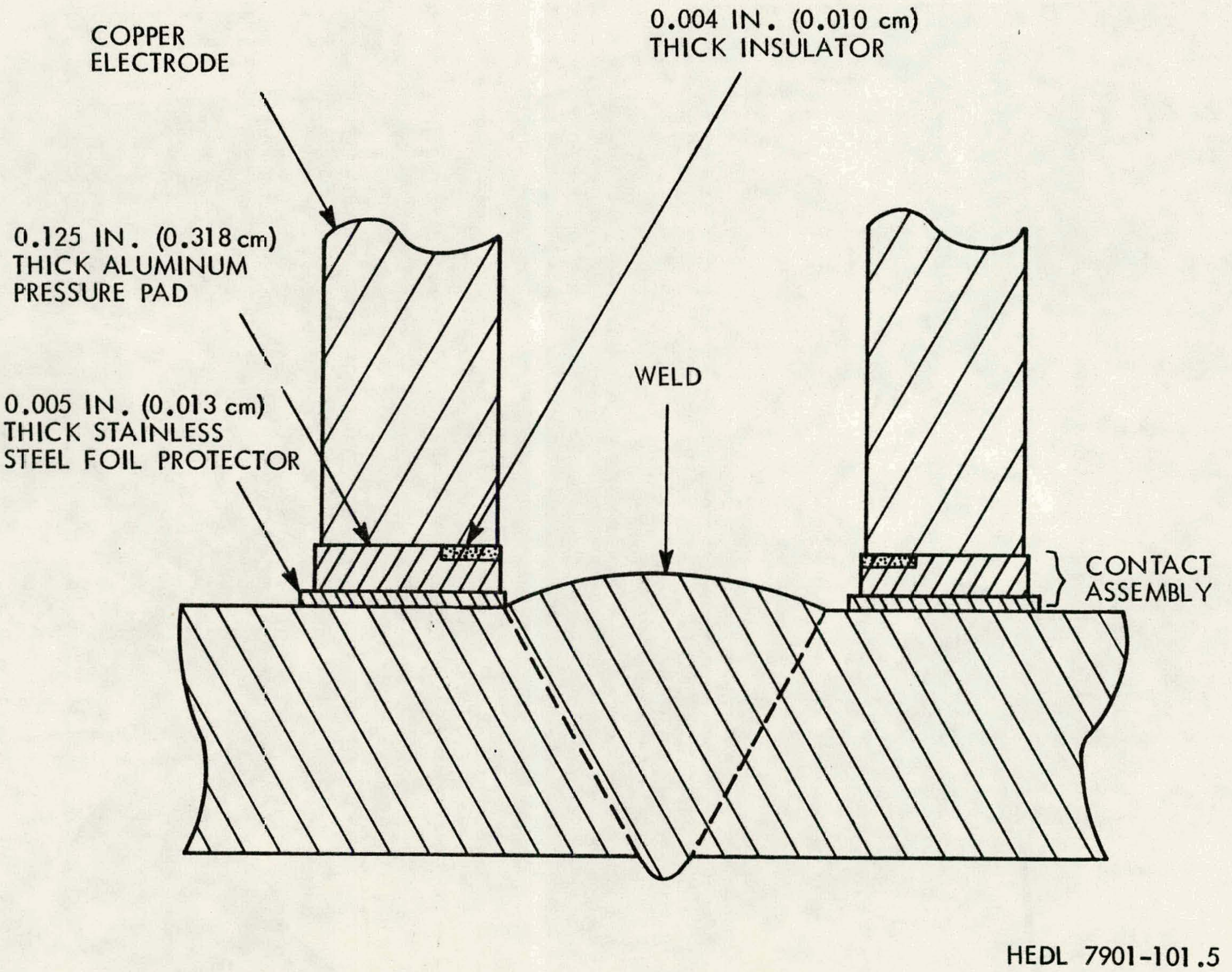

Figure 6. Cross section showing electrode and contact assembly in place ready for electro-thermal NDT of a pipe weld.

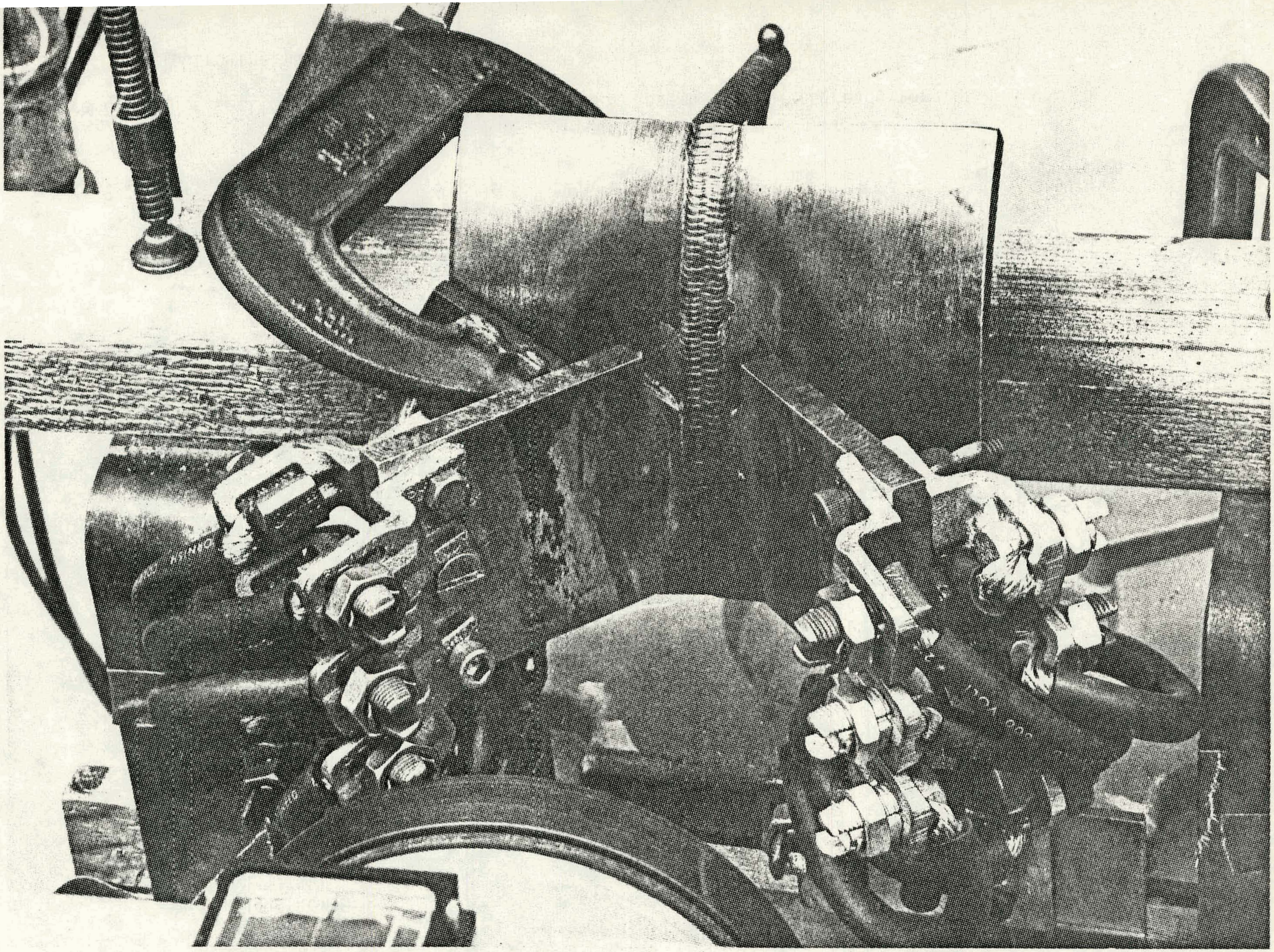

Figure 7. Front view of the stainless steel pipe weld specimen with early soldered-on electrodes used to collect comparison data. This specimen is from a 14 inch (36cm) diameter pipe.

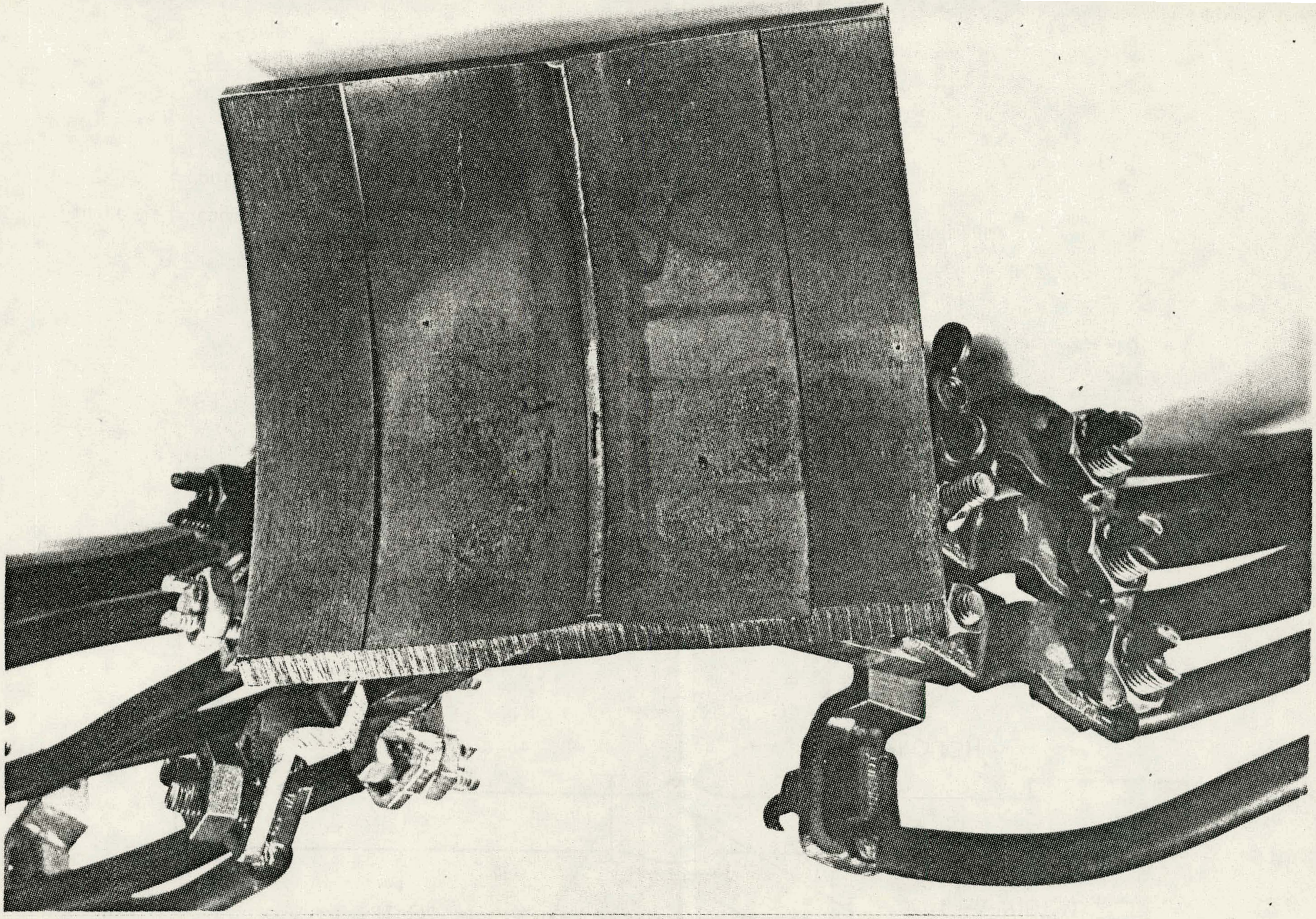

Figure 8. Rear view of the stainless steel pipe weld specimen and electrode assembly showing the electro-discharge machined weld defect.

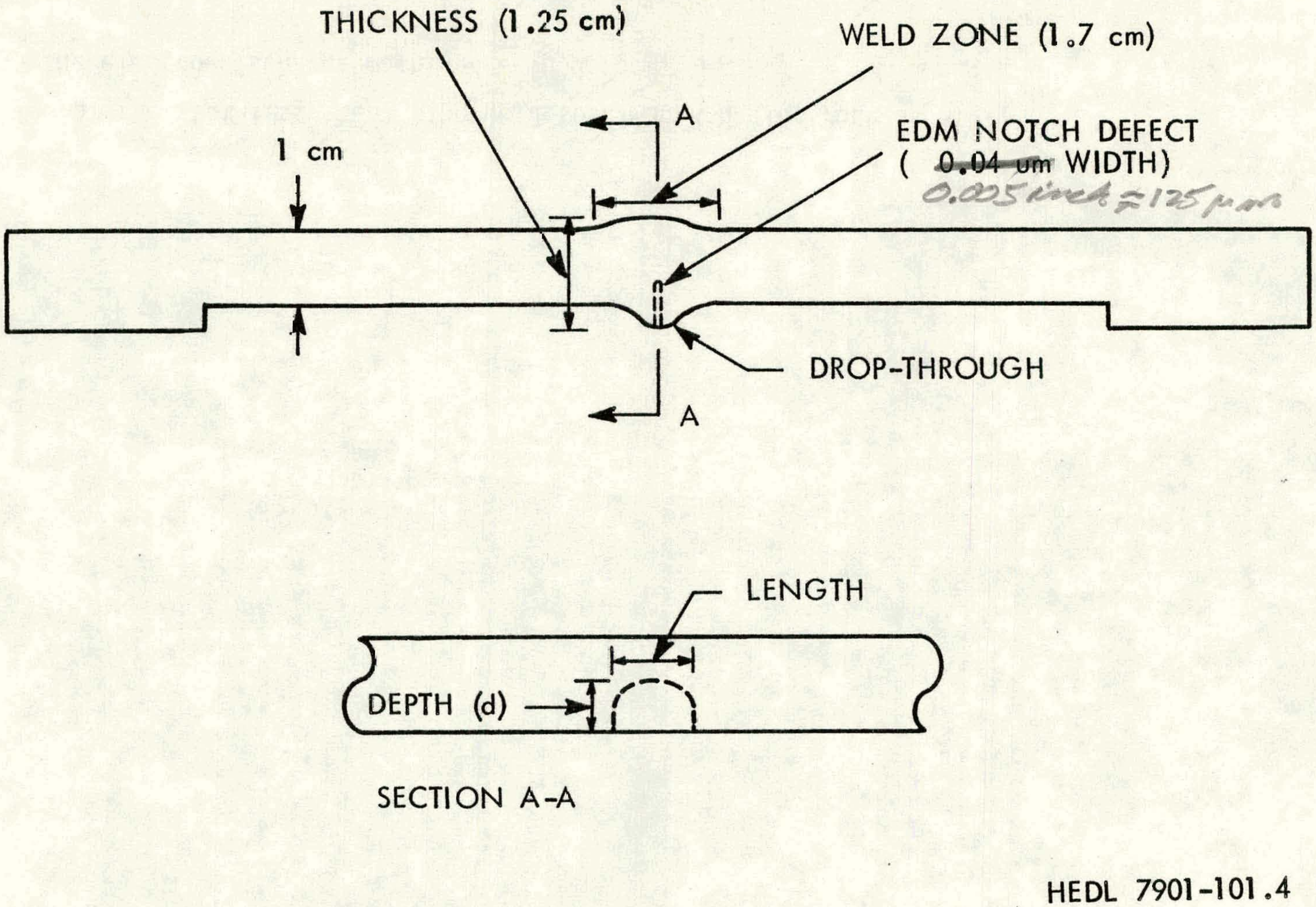

Figure 9. Schematic cross sectional diagram of the stainless steel weld specimens containing electro-discharge machined defects.

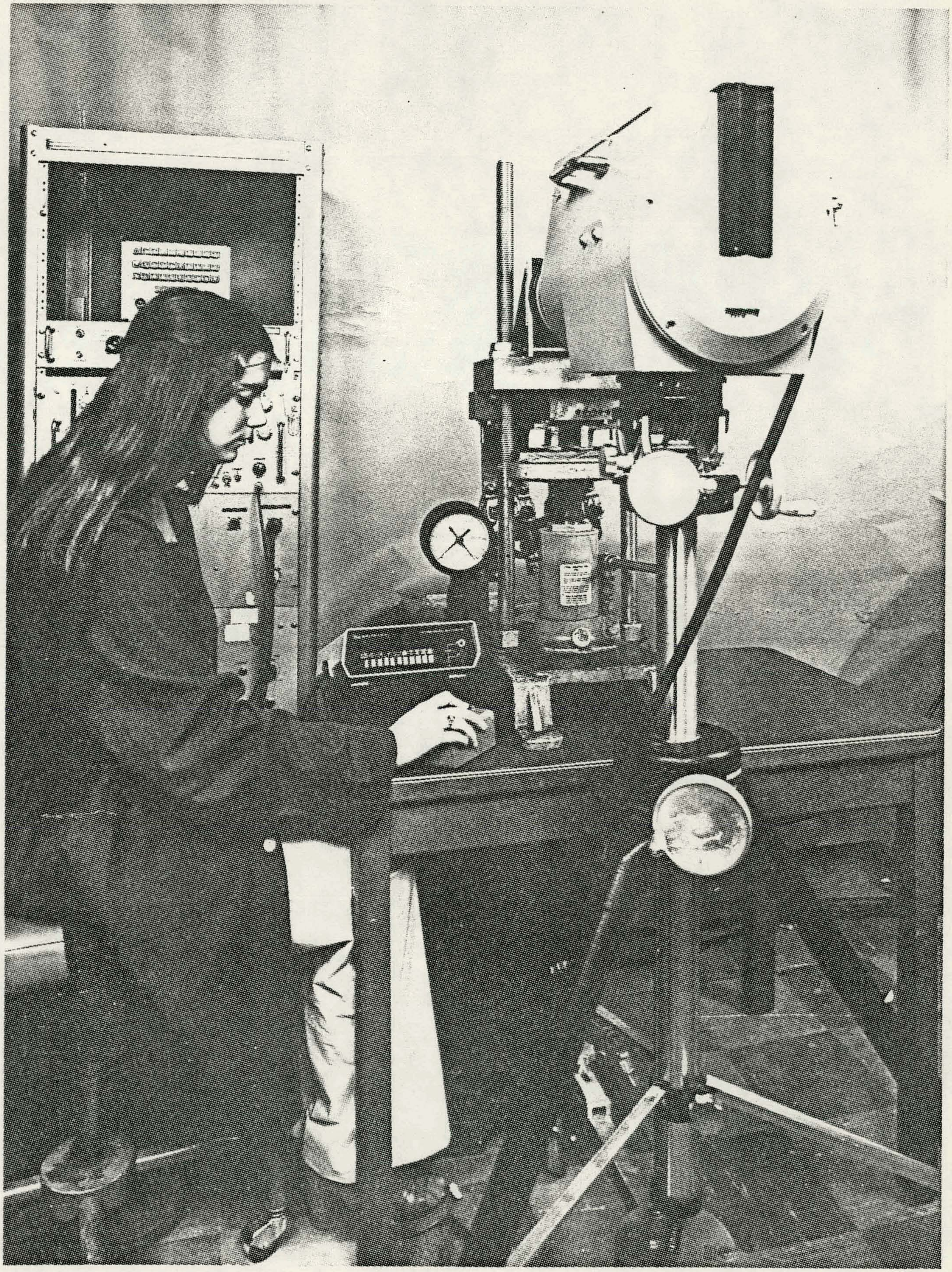

Figure 10. Electro-thermal apparatus for experiments using flexible non-bonded contacts on stainless steel pipe weld specimens.

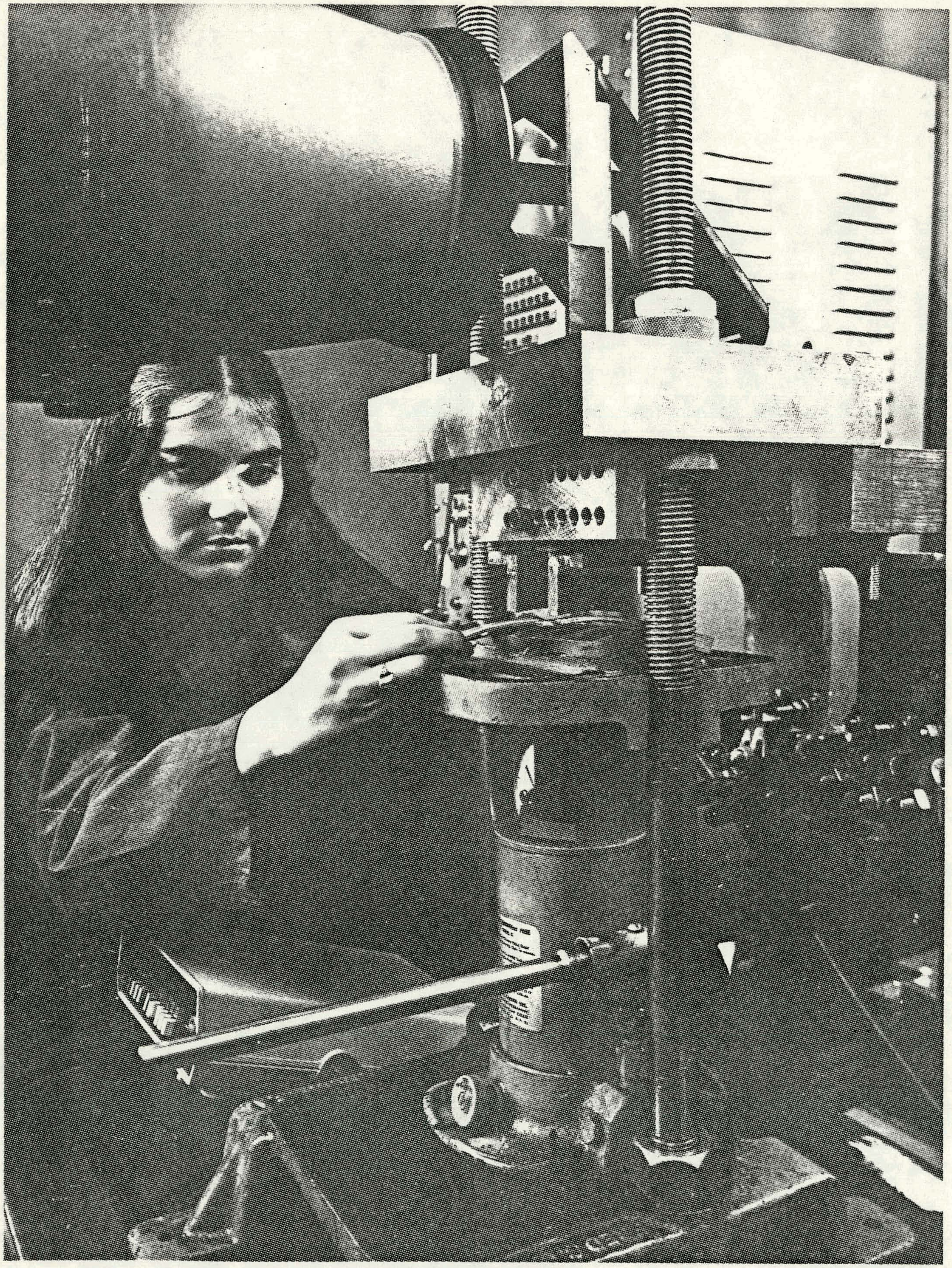

Figure 11. Operator is inserting a flexible contact assembly under one of the electrodes.

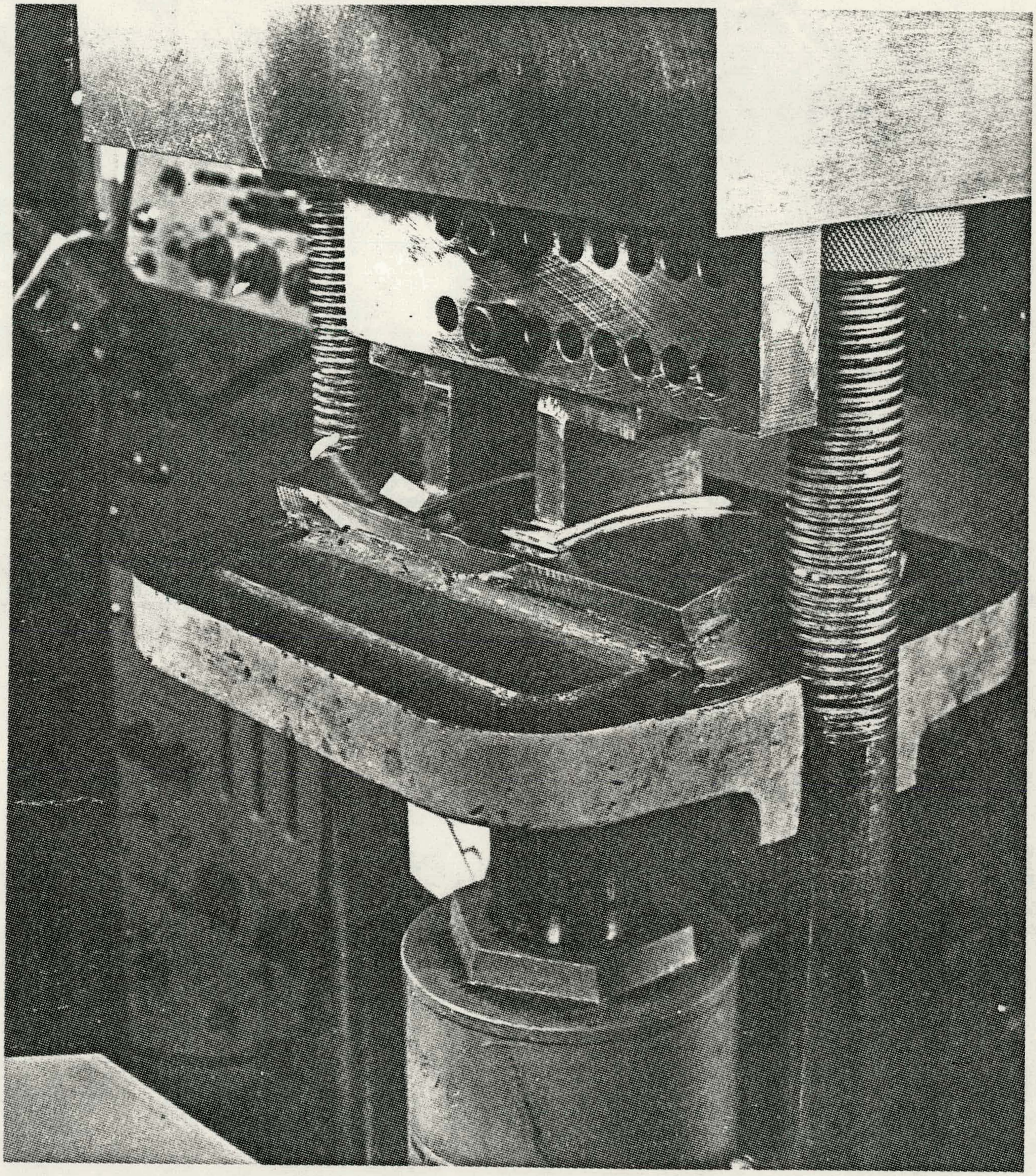

Figure 12. Electrodes and contact assemblies in-place and ready for electro-thermal NDT of a stainless steel pipe weld specimen.

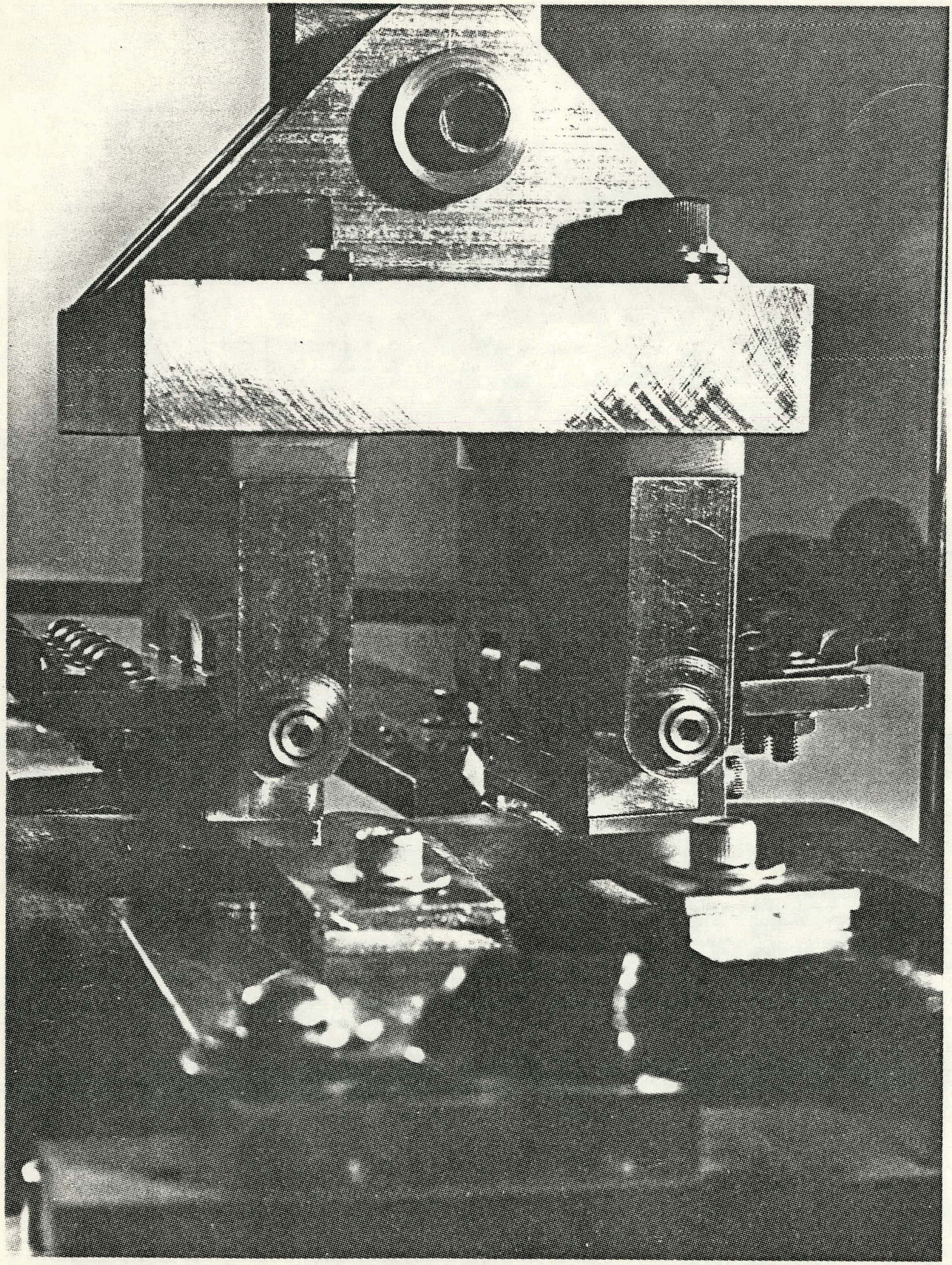

Figure 13. Swivel electrodes and heated contact assembly.

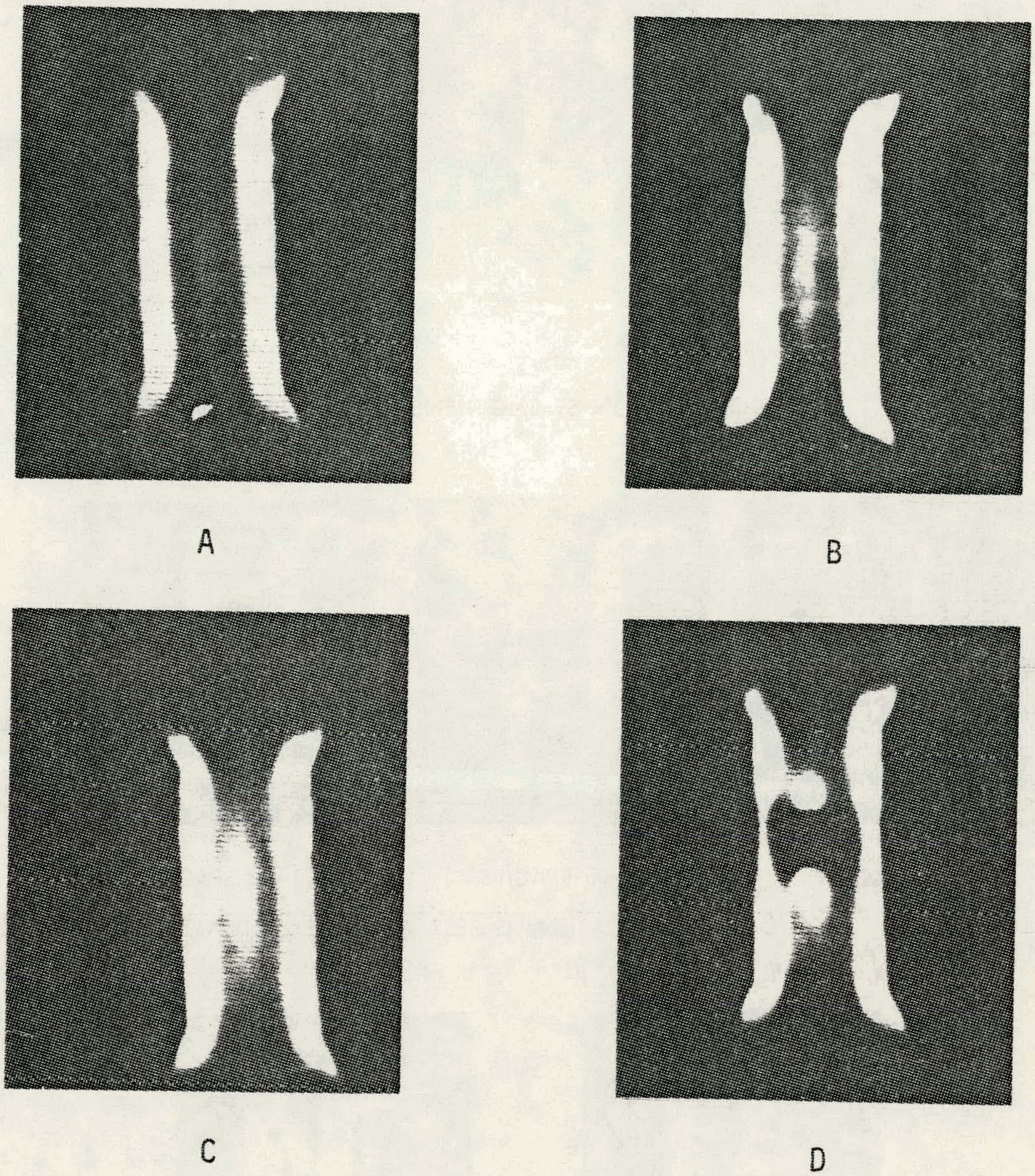

Figure 14. (A) Background Electro-Thermal Map on Stainless Pipe Weld Sample (No Flaws).

(B) Electro-Thermal Map on Same Weld as (A), but With 43% Flaw.

(C) Electro-Thermal Map on Same Weld as (A), but With 66% Flaw.

(D) Electro-Thermal Map on Same Weld as (A), but With 100% Flaw.

DEFECT INDICATION

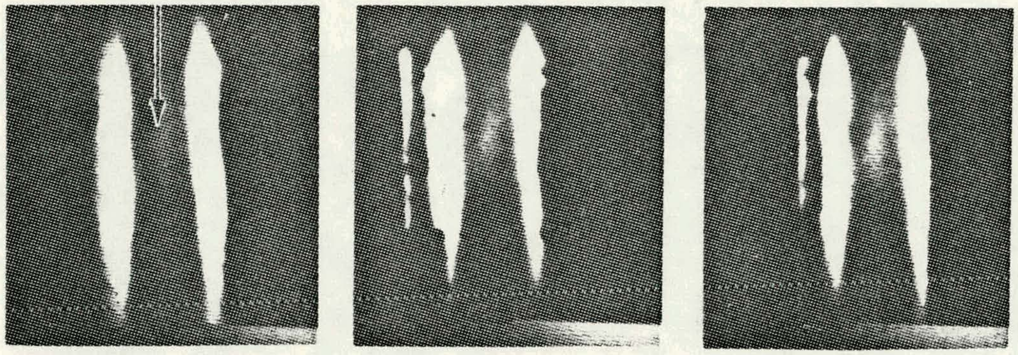

DEPTH = 20% 40% 50%

Figure 15A. DEFECT INDICATION STRENGTHENS WITH INCREASING DEPTH

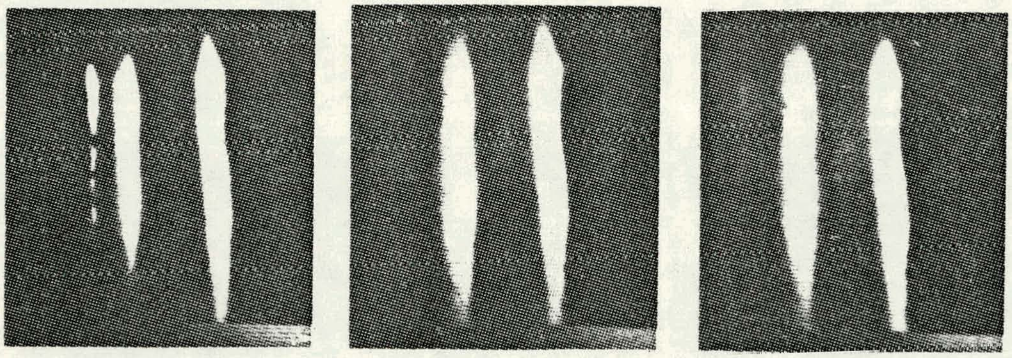

3-cm SPACING 3.8-cm SPACING 5.1-cm SPACING

Figure 15B. 20% DEFECT INDICATION IS BEST WITH APPROXIMATELY 3.8 cm ELECTRODE SPACING

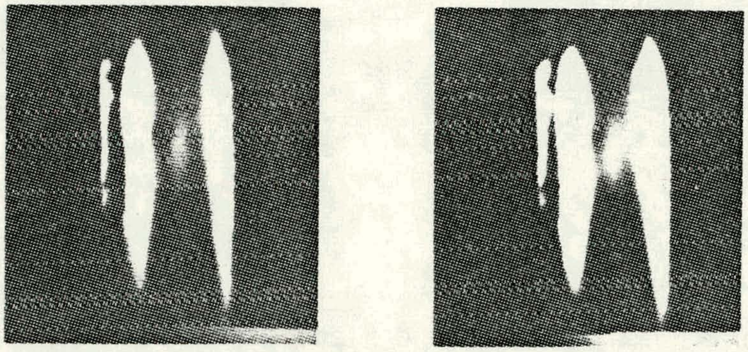

3.8-cm SPACING 2.5-cm SPACING

Figure 15C. 50% DEFECT INDICATION IMPROVES WITH SHORT ELECTRODE SPACING

Figure 15. Electro-thermal NDT results obtained using a non-bonded contact on a stainless steel pipe weld specimen cut from a 14 inch (36 cm) diameter pipe.